



Insight into human protease activated receptor-1 as anticancer target by molecular modelling

A.N. Hidayat, E. Aki-Yalcin, M. Beksac, E. Tian, S.Z. Usmani, T. Ertan-Bolelli & İ. Yalcin

To cite this article: A.N. Hidayat, E. Aki-Yalcin, M. Beksac, E. Tian, S.Z. Usmani, T. Ertan-Bolelli & İ. Yalcin (2015) Insight into human protease activated receptor-1 as anticancer target by molecular modelling, SAR and QSAR in Environmental Research, 26:10, 795-807, DOI: 10.1080/1062936X.2015.1095799

To link to this article: <http://dx.doi.org/10.1080/1062936X.2015.1095799>



Published online: 26 Oct 2015.



Submit your article to this journal [↗](#)



Article views: 14



View related articles [↗](#)



View Crossmark data [↗](#)

Insight into human protease activated receptor-1 as anticancer target by molecular modelling†

A.N. Hidayat^a, E. Aki-Yalcin^{b*}, M. Beksac^c, E. Tian^d, S.Z. Usmani^e, T. Ertan-Bolelli^b and İ. Yalcin^b

^aBioinformatics Department, Ankara University, Ankara, Turkey; ^bPharmaceutical Chemistry Department, Ankara University, Ankara, Turkey; ^cInternal Medicine Department, Ankara University, Ankara, Turkey; ^dMyeloma Institute, University of Arkansas for Medical Sciences, Arkansas, USA; ^eLevine Cancer Institute, Carolinas Healthcare, Charlotte, USA

(Received 22 June 2015; in final form 15 September 2015)

Protease-activated receptor 1 (PAR1) has been established as a promising target in many diseases, including various cancers. Strong evidence also suggests its role in metastasis. It is proved experimentally that PAR1 can induce numerous cell phenotypes, i.e. proliferation and differentiation. A strong link between PAR1 gene overexpression and high levels of β -catenin was suggested by a study of the PAR1– $G\alpha(13)$ –DVL axis in β -catenin stabilization in cancers. An in vitro study was carried out to analyze PAR1 expression by flow cytometry on CD38+138+ plasma cells obtained from patients either at diagnosis (n : 46) (newly diagnosed multiple myeloma (NDMM)) or at relapse (n : 45) (relapsed/refractory multiple myeloma (RRMM)) and compared with the controls. Our previously synthesized benzoxazole (XT2B) and benzamide (XT5) derivatives were tested with in vitro 3-(4,5-dimethylthiazol-2-yl)-2,5-diphenyltetrazolium bromide (MTT) assays, which revealed significant inhibitory activity on PAR1. We provide docking studies using Autodock Vina of these newly tested compounds to compare with the known PAR1 inhibitors in order to examine the binding mechanisms. In addition, the docking results are validated using HYDE binding assessment and a neural network (NN) scoring function.

Keywords: anticancer; benzamide; benzoxazole; molecular docking; PAR1 antagonist

1. Introduction

Protease-activated receptors (PARs) are part of the large seven-transmembrane-spanning G protein-coupled receptor (GPCR) family, shown to couple to $G_{i/o}$, G_q or $G_{12/13}$ within the same cell type [1]. Of the 16 G protein genes found in the mammalian genome, the subfamily member G_{12} is of the most interest to cancer biologists. G_{12} and its sister family member, G_{13} , are the only G proteins that have the capability to transform fibroblasts on the overexpressed condition in their wild-type (WT) form. Recent studies have demonstrated that G_{12} is markedly up-regulated in adenocarcinoma of the breast and have identified the G_{12} protein as an important indicator of breast and prostate cancer invasion. The G_{12} protein subunit also plays a role in disrupting the cadherin–catenin interaction and down-regulation of the extracellular cell-cell adhesive function of cadherins [2].

*Corresponding author. Email: esinaki@ankara.edu.tr

†Presented at the 8th International Symposium on Computational Methods in Toxicology and Pharmacology Integrating Internet Resources, CMTPI-2015, 21–25 June 2015, Chios, Greece.

PARs are normally activated by the proteolytic exposure of an occult tethered ligand [3]. There are four family members of this protein (PAR 1–4), and the one most characterized is protease-activated receptor 1 (PAR1) [4]. PAR1 receptor is activated by coagulation protease thrombin via specific cleavage of the *N*-terminal exodomain of the receptor to generate a new *N*-terminus. This *N*-terminus then remains attached to the receptor and function as a ligand, called a tethered ligand (TL), and triggers conformational changes of the receptor resulting in G-protein activation at the end of signalling cascades [4–7].

PAR1 has been established as a promising target in many diseases including various cancers. It has been reported that there is an increasing level of expression of this protein in many cancer conditions such as breast cancer [8], colon cancer [9] and prostate cancer [10]. Although the clear role of the PAR1 mechanism in cancer is not completely understood, it has been proved experimentally that PAR1 can induce numerous cell phenotypes, i.e. proliferation and differentiation of multiple myeloma (MM) conditions [11]. Increased expression of PAR1 is correlated with a malignant phenotype, and its role has been proved in various cancers, namely breast, colon, kidney, pulmonary tumour and hepatocellular carcinoma [12]. Enhanced expression of PAR1 was observed in invasive and metastatic tumours and, interestingly, the expression levels directly correlated with the degree of invasiveness of the cancer [13, 14].

In addition, strong novel evidence has shown a link between PAR1 gene overexpression and high levels of β -catenin, in a study of the PAR1– $G\alpha(13)$ –DVL axis in β -catenin stabilization in cancers [15, 16]. Mutations and overexpression of β -catenin are mainly associated with many cancers, such as hepatocellular and colorectal carcinomas, lung cancer and malignant breast tumours, as well as ovarian and endometrial cancers [17]. Thus, PAR1 is a potentially important therapeutic target for the treatment of various cancers, with scarce data on potential antagonists.

Computational methods have become a routine method during the drug discovery process, in which molecular docking is one of the important techniques for accelerating the process [18]. Making a prediction of the ligand–receptor complex structure is the main role of computational methods that use molecular docking. Docking can be achieved through two important steps: first by sampling conformations of the ligand in the binding pocket of the protein; then ranking these conformations via a scoring function. Sampling algorithms are used to reproduce the experimental binding mode and the scoring function is then used to rank the highest of the generated conformations [19]. AutoDock Vina tools (hereinafter referred as Vina) is a successor to the most cited docking program AutoDock, which showed approximately two orders exponential improvement of magnitude in speed and a significantly better accuracy for making ligand–receptor complex binding mode predictions [20]. The prediction of binding affinity calculated from a docking program alone sometimes creates false-positive or false-negative results. To obtain more precise results, re-scoring is needed, using a more robust scoring function and adding empirical calculations to mimic the real system. The neural network scoring function (NNScore) is a knowledge-based scoring function that utilizes a computational method mimicking the neural network of the human brain, and is suitable for re-scoring AutoDock Vina results [21]. Moreover, two major contributions of the binding energy, which are hydrogen bonding and the hydrophobic effect, as well as the unfavourable contribution of hydrophilic dehydration, becoming important for better free-energy-binding estimation. With this aim, the HYDE scoring function, based on consistent dehydration energies and a description of the hydrogen bond in protein–ligand complexes, is suitable for validating the results of docking predictions [22].

Benzoxazole and benzamide compounds, which had previously been synthesized in our laboratory [23, 24], showed a strong inhibitory activity for human DNA topoisomerases and glutathione transferases P1-1, and anticancer effects were also observed on various cell cultures [25]. Thus, these might exhibit a similar anticancer action upon a new target, PAR1.

In this research, we took our previously synthesized compounds (XT2B, XT5) [23, 24] and tested them with an 3-(4,5-dimethylthiazol-2-yl)-2,5-diphenyltetrazolium bromide (MTT) assay to find their antagonist activity against PAR1 [15]. Our previous studies determined that compounds possessing similar structures to these compounds had indicated several anticancer effects on various cancer cell lines [25].

To provide an insight into the binding mechanisms, we made docking studies of these new test compounds against the PAR1 receptor to propose new anticancer drug candidates. The docking study was as follows: (1) re-docking of the antagonist Vorapaxar–PAR1; (2) docking of another antagonist against PAR1; (3) calculating the free energy binding estimation using the HYDE program and NN scoring function; and (4) visualization of all the binding poses.

2. Material and methods

2.1 Experimental *in vitro* assays

In this study, we analyzed PAR1 expression (WEDE15 PE, Beckman Coulter, Fisher Scientific, Pittsburg, USA) by flow cytometry, on CD38+138+ plasma cells obtained from patients either at diagnosis (n : 46) (newly diagnosed multiple myeloma (NDMM)) or at relapse (n : 45) (relapsed/refractory multiple myeloma (RRMM)) and compared the results with the controls. Human myeloma cells RPMI 8226 were grown in RPMI 1640 medium supplemented with 10% fetal bovine serum, penicillin (100 U/mL), and streptomycin (100 mg/mL) in a 5% CO₂ atmosphere at 37°C. Sterile bovine serum was inactivated at 60°C for 30 min before preparing the medium. The cells were stained with trypan blue and counted to seed an equal number of cells to each well of the 96-well plates.

The compounds were dissolved in dimethyl sulfoxide (DMSO) and kept as 20 mM stock solutions at –20°C, protected from light. In none of the experiments did the DMSO concentration exceed 0.5%, which did not interfere with cell growth.

The molecules were tested in tert-butyl(2S)-2-(pyrrolidin-1-ylcarbonyl)pyrrolidine-1-carboxylate (UAMC) for MTT assay on primary and Bortezomib refractory cell lines. Eleven anti-PAR1 molecules tested by *in vitro* MTT assay. The MTT test was used to determine cell viability. Briefly, the cells (2×10^4 per well) were seeded into 96-well plates and their proliferation was determined with the Cell Proliferation Kit I (Roche, Mannheim, Germany) as described by the manufacturer. The cells were treated at various concentrations (0.1, 1, 10, 20, 30, 40, 50, 75 and 100 μ M) of the newly synthesized compounds for 72 h. The spectrophotometric absorbance was measured using a microplate reader at 550 nm with a reference wavelength of 690 nm. Data were expressed as percentage cell viability against the untreated control. DMSO was used as negative control in the corresponding concentrations.

2.2 Retrieval of protein 3D structure

Protein Data Bank (PDB) ID 3VW7 represents the 2.2 Å resolution crystal structure of human PAR1 bound to Vorapaxar, a PAR1 antagonist [26]. The structure was retrieved from Brookhaven Protein Data Bank (<http://www.rcsb.org/pdb>). Only the structure corresponding

to the transmembrane region was considered in our studies. The crystal structure was prepared for docking analysis after removing water and the co-crystallized ligand, Vorapaxar.

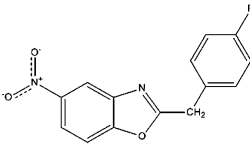
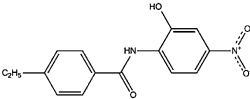
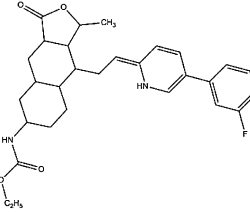
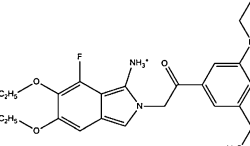
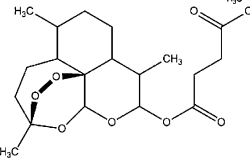
2.3 Retrieval of the ligands' 3D structures

The ligands' 3D structures used for this analysis were obtained from our research group, containing derivatives of benzoxazole (XT2B) and benzamide (XT5). For a comparative study, we also use structures of Vorapaxar, Atopaxar and Artesunate retrieved from Zinc databases [27] (Table 1).

2.4 Preparations of the protein and the ligands

The crystal structure of PAR1 was prepared using the protein preparation wizard of Biovia Discovery Studio 3.5 [28]. The protein preparation wizard prepares the structures by adding missing hydrogen atoms and correcting bond order assignments, charge states and orientation of various groups. This was done to improve charge–charge interactions with neighbouring groups. The final step in protein preparation was minimization using the adopted-basis Newton-Raphason (ABNR) method with the Chemistry at Harvard Molecular Mechanics (CHARMM) force field. All of the ligand structures were prepared using a similar protocol.

Table 1. Structures of ligand for the PAR1 docking study.

Number	Ligand name	2D structures
1	XT2B compound	 2-(4-fluoro-phenyl)-methyl-5-nitro benzoxazole
2	XT5 compound	 <i>N</i> -(2-hydroxy-4-nitro-phenyl)-4-ethyl benzamide
3	Vorapaxar	
4	Atopaxar	
5	Artesunate	

2.5 Molecular docking and validation

In order to distinguish the possibility of interaction between the receptor and certain ligands, molecular docking was performed. We used the Autodock/Vina plugin for PyMOL [29], which is very useful for defining binding sites, preparing receptors and ligands, generating grid files, setting up docking runs and showing the binding pose of docking directly in the PyMOL [30] visualization environment for performing the molecular docking process. In the docking workflow, receptor grid generation was centred on the following residues: TYR337, A349, L340, H255, L258 and H336, and the water molecules around that area that still remain intact (Figure 1(a)). These residues were identified as important residues for binding in the crystal structure of PAR1 [26]. The docking study was conducted as follows: (1) redocked Vorapaxar–PAR1; (2) docking another ligand against PAR1; (3) calculation of free energy binding estimate using the HYDE program and the NN scoring function. All of the binding poses were then visualized using Biovia Discovery Studio visualizer [28].

3. Results and discussion

Some benzoxazole and benzamide compounds, which had previously been synthesized in our laboratory [23, 24], were tested by *in vitro* MTT assay and revealed significant inhibitory activity on PAR1. We provide docking studies of these new novel test compounds for comparison with the known PAR1 inhibitors using Autodock Vina, in order to examine the binding mechanisms.

PAR1 is expressed by plasma cells at different levels for myeloma patients at diagnosis and relapse. The research was conducted on the activity of some novel compounds, with variations in structure, that had previously been synthesized by our group (Table 1). We carried out an *in vitro* study to analyze PAR1 expression by flow cytometry on CD38+138+ plasma cells obtained from patients either at diagnosis (n : 46) (NDMM) or at relapse (n : 45) (RRMM) and compared with the controls. Expression was found at greater than the levels observed among normal marrow plasma cells. PAR1 expression did not correlate with International Staging System (ISS) age, Lactate Dehydrogenase (LDH), fluorescence *in situ* hybridization (FISH), marrow plasma cell percentage or response to treatment. Of the eleven anti-PAR1 molecules tested by *in vitro* MTT assay, XT5 and XT2B were found to have the lowest IC₅₀ concentrations (Table 2). The IC₅₀ values were similar on the human myeloma cell lines (HMCLs) and not correlated with the level of PAR1 expression.

The new PAR1 binding molecules have *in vitro* anti-myeloma cytotoxic effects on both primary and Bortezomib refractory cell lines. Treatments containing Bortezomib have been shown to enhance heparanase activity, leading to resistance. These molecules might exert their activities by blocking downstream effects of heparanase. As a result of MTT assays, XT2B and XT5 were found to have significant PAR1 inhibitory activities (Table 2).

We carried out comparative docking studies of the high-resolution crystal structure of human PAR1 (PDB: 3VW7) [23] against known inhibitors and our novel test compounds using Vina tools [20]. In addition, the results were also validated by using NNScore [21] and the HYDE binding assessment scoring function [22].

Before the docking calculation was performed, we analyzed the physico-chemical properties of the ligands to check their drug-likeness factor, Lipinski's rule of five (RoF), which is one of the most used criteria [31]. Another criterion used for drug-likeness analysis is the Veber rules, which are important for oral bioavailability [32]. The physico-chemical properties of the ligands used in the PAR1 docking study, which were calculated using Biovia Discovery

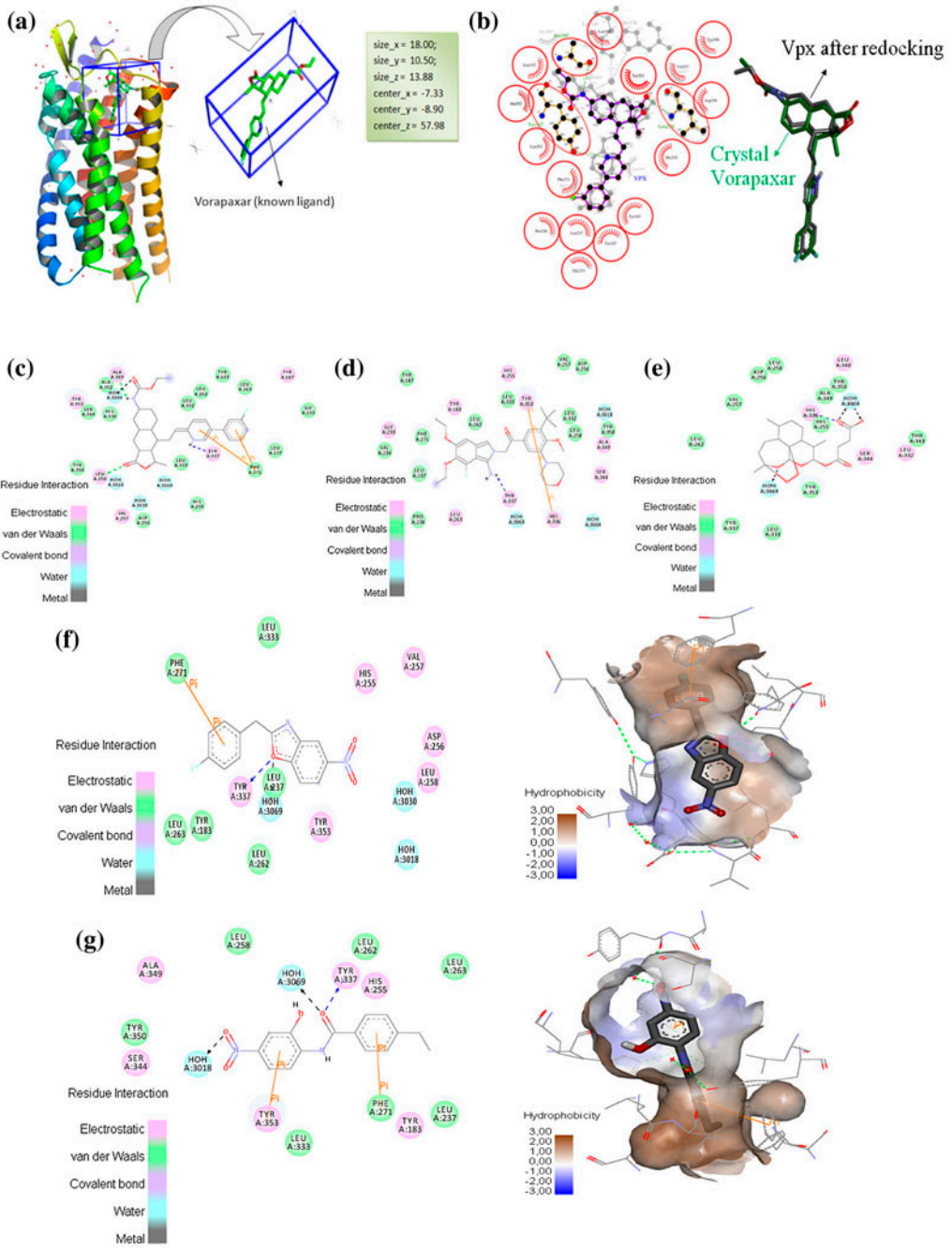


Figure 1. (a) Grid box used for docking calculation using Autodock Vina. (b) Result of the comparison of binding interactions of Vorapaxar with the PAR1 crystal structure and the Autodock Vina. Docking score = -13.3 kcal/mol, RMSD = 0.790 Å. (c-g) Binding interactions of human PAR1 with ligands. (c) Vorapaxar; (d) Atopaxar; (e) Artesunate; (f) XT2B; (g) XT5. Pink, electrostatic interaction; green, van der Waals; blue, water interaction; blue arrow, hydrogen bond donor interaction; green arrow, hydrogen bond acceptor interaction; black arrow, hydrogen bond interaction within water molecule; orange line, Pi stacking interaction. Hydrophobicity representation shows ligands in the PAR1 binding pocket. It is suggested that amino acid residue TYR337 is an important amino acid for further studies.

Table 2. IC₅₀ concentrations of compounds from in vitro MTT assay.

Cell lines	XT5 [μ M]	XT2B [μ M]
U266BR	7.2	16.33
U266	7.92	34.7
JJN3BR	6.17	21.82
JJN3	7.5	11.51
H929R	8.12	33.89
OPM2	6.5	25.75
OPM2R	7.89	30.18
KMS28PE	10.7	41.42

The results of the MTT assays indicated that XT2B and XT5 were found to have significant inhibitor activities in PAR1 inhibition assays.

Table 3. Physico-chemical properties of ligands used in the Biovia Discovery Studio 3.5 docking calculation.

Number	Ligands	AlogP	MW	HA	HD	ROTB	Number of rings	Number of aromatic rings	Molecular PSA
1	Vorapaxar	4.273	494.598	5	2	6	5	1	76.66
2	Atopaxar	4.308	528.635	7	1	10	4	2	86.06
3	Artesunate	0.371	383.413	8	0	5	4	0	103.35
4	XT2B	3.311	273.239	3	1	3	3	3	70.40
5	XT5	3.105	287.291	4	3	4	2	2	93.69

AlogP, lipophilicity; MW, molecular weight; HA, number of hydrogen acceptor; HD, number of hydrogen donor; ROTB, rotatable bonds; Molecular PSA, molecular polar surface area.

Studio 3.5 Molecular Properties Calculation method, are shown in Table 3. After obtaining all of the important properties for these ligands such as molecular weight (MW), lipophilicity (AlogP), number of hydrogen acceptor (HA), number of hydrogen donor (HD), rotatable bonds (ROTB), number of rings, number of aromatic rings and molecular polar surface area (PSA), we filtered the ligands based on Lipinski's rule of five and Veber's rule, with parameters for the number of violations tolerated set to one violation (based on Lipinski's original paper) [31]. The results reported that all of the ligands passed Lipinski's and Veber's rules. The ligands passing the filters have a higher probability of good oral bioavailability. Thus, all of these compounds have the potential to act as drugs on the human body.

We then examined the binding affinity of the novel test compounds, benzoxazole and benzamide derivatives, on PAR1 and also compared the results with known PAR1 antagonists such as Vorapaxar, Atopaxar and Artesunate, anti-malarial drugs that have effects as anticancer agents on multiple myeloma (MM). As the compounds showed strong inhibitory activities for human DNA topoisomerases and glutathione transferases P1-1, as well as anti-cancer effects on various cell cultures [25], they have also been determined to have a similar anticancer action upon the new target PAR1.

Molecular docking (MD) is a computational procedure that attempts to predict noncovalent binding of macromolecules or, of a macromolecule (receptor) and a small molecule (ligand) efficiently more frequently, starting with their unbound structures, homology modelling or structures obtained from MD simulations. The goal is to predict the binding affinity and the bound conformations. A molecular docking technique was performed for this study using Vina to analyze the binding pose of ligands against the PAR1 receptor. The docking

program is publically well-known, most cited and has good accuracy results while performing in silico molecular docking studies [20]. The docking workflow started with a re-docking method between co-crystallized PAR1 and its ligand, Vorapaxar. The re-docked result showing a significant similarity with the crystal structures of PAR1 bound to Vorapaxar (PDB: 3VW7) with an RMSD score of 0.790 Å and a docking score of 13.3 kcal/mol (Figure 1(b)). The re-docking calculation is important because when a re-dock returns a binding pose deviation or RMSD closer to that of the crystal one (<2.0 Å) or has binding interactions with certain amino acids similar to the crystal one, it means that the docking system is ready to use for other molecules or ligands. As described in Figure 1(b), the circles and oval marks refer to the similar amino acids that have the same binding interactions both in the crystal structure and the Vina re-docking result. While circular marks refer to non-bonded interactions, the oval marks with certain amino acids show the hydrogen interactions with the receptor. Hydrogen bonds within Vorapaxar and the receptor, both in the crystal structure and Vina re-docked results are: TYR337, LEU258, ALA349 and water molecule HOH3004. Other hydrogen bonds are from the water molecule HOH3004 with LEU340 and HIS336 (Table 4). This re-docked result has -13.0 kcal/mol of binding affinity as calculated with Vina.

Based on the re-dock study between Vorapaxar and PAR1 receptor, which shows a good result, we used its docking system information to perform molecular docking calculations with other ligands. Docking results using Autodock Vina against the PAR1 receptor for all of the ligands are shown in Table 4. The results indicate that Vorapaxar has the highest docking score while Atopaxar has the lowest docking score among other ligands. Even the known antimalaria drug Artesunate has a quite good docking score.

Benzoxazole (XT2B) and benzamide (XT5) compounds, which had previously been synthesized in our laboratory, showed promising docking scores based on the Vina program when compared to known antagonists of PAR1, where XT2B has -9.1 kcal/mol and XT5 has -9.9 kcal/mol for their binding affinity calculations. Noncovalent interactions between PAR1 receptor and its docked ligands based on the Autodock Vina binding pose have various results. The observed hydrogen bond donor residue from PAR1 that interacts with the most ligands is TYR337. Re-docked Vorapaxar binding interactions have similar results to the PAR1 crystal bound to Vorapaxar structure (PDB: 3VW7). It has three hydrogen bond interactions, as with TYR337, LEU258 and ALA349, and it also interacts with one water molecule (HOH3004-LEU340, HIS336). Atopaxar has hydrogen bond interaction with hydrogen bond donor residue TYR337. Meanwhile, Artesunate has interaction with hydrogen bond acceptor HIS336 and two water molecules that also interact with other residues within the PAR1 receptor ((HOH3004-LEU340) and (HOH3069-THR261, LEU262, TYR337)). Our new molecules that were tested, XT5 and XT2B, also have similar hydrogen bond interactions. Molecule XT5

Table 4. Docking results for the PAR1 receptor using Autodock Vina.

Number	Ligands	Docking score E_{bind} (kcal/mol)	Amino acid interactions (van der Waals contact distance <4 Å)
1	Vorapaxar	-13.3	TYR337, LEU258, ALA349, (HOH3004-LEU340, HIS336)
2	Atopaxar	-8.0	TYR337
3	Artesunate	-9.6	HIS336, (HOH3004-LEU340), (HOH3069-HR261, LEU262, TYR337)
4	XT5	-9.9	TYR337, (HOH3069-HIS336, THR261, LEU262, TYR337), (HOH3018-ASP256, TYR95, TYR350)
5	XT2B	-9.1	TYR337

interacts with TYR337, acting as a hydrogen bond donor and two water molecules ((HOH3069-HIS336, THR261, LEU262, TYR337) and (HOH3018-ASP256, TYR95, TYR350)), while molecule XT2B has just one hydrogen bond interaction with TYR337. Our results reveal that TYR337 is an important residue that could be targeted for further studies correlating the structure–activity relationships (Figure 1(c)–(g)).

Zhang et al. reported that the TYR337 residue, which is located at the carboxy-terminal end of trans-membrane 6 (TM6) region of PAR1, had a strong hydrogen bond with the pyridine ring of Vorapaxar [26]. Together with other amino acid residue interactions, noncovalent interaction of the TYR337 residue might influence ligand-binding selectivity indirectly by contributing to the overall structure and stability of the PAR1 receptor binding pocket. Mutation of TYR337 to PHE337 led to a reduction in cell surface expression, making it difficult to interpret the associated reduction in agonist peptide activation of the PAR1 receptor. Hydrogen bonds, in terms of ligand binding have at least three different functions, such as: (1) contributing to the conformational changes of the ligand by its binding partner; (2) having a recognition function to distinguish between agonist, antagonist, substrate or inhibitors; and the important one is (3) contributing to ligand-binding affinities against its receptor [33]. So, hydrogen bonds are very important for make sure that certain compounds maintain their ability to interact with the receptor and can, in the end, initiate further molecular action.

Current scoring functions for docking prediction can be divided into three general categories [34]. The first category, based on molecular force fields, predicts binding energy by estimating electrostatic and van der Waals forces explicitly, for which Autodock uses this kind of scoring function. A second category is known as empirical scoring functions, which estimate binding energy by calculating the weighted sum of all hydrogen-bond and hydrophobic contacts. A third category of the scoring function, called as ‘knowledge based’, relies on statistical analyses of crystal-structure databases. Pairs of atom types that are frequently found in close proximity are judged to be energetically favourable. These approaches to binding-affinity prediction have proven very useful.

To get more accuracy from the docking calculation, it needs to estimate the free energy of binding, which becomes an important parameter for deciding the best docking pose. For this purpose, we used NNScore, based on a neural network; a computational model that attempts to simulate the microscopic organization of the brain and suited for use with Autodock Vina [21] and also the HYDE scoring function that is based on a consistent description of hydrogen bond and dehydration energies in protein–ligand complexes [22].

We used the NNScore program, based on a fast and accurate neural network algorithm, to re-score the current PAR1 docking score results (Table 5). The binding score provided by NNScore is associated with the best ranking among the average scores for the model from 20 networks that were generated during calculation. Along with the re-score function, NNScore also estimates the dissociation constant (K_d), which is important for distinguishing between good and poor binders. Protein–ligand complexes that have a dissociation constant $K_d < 25 \mu\text{M}$

Table 5. Re-score values and predicted K_d (dissociation constant) provided by NNScore.

Number	Ligands	Model	NNScore	STD	Predicted K_d
1	Vorapaxar	Model 1	9.877	2.046	132.86 pM
2	Atopaxar	Model 2	6.219	2.678	603.31 nM
3	Artesunate	Model 2	6.976	1.517	105.58 nM
4	XT5	Model 7	7.590	2.767	25.70 nM
5	XT2B	Model 7	7.779	3.618	16.63 nM

indicates good binders, while protein–ligand complexes that have a dissociation constant $K_d > 25 \mu\text{M}$ indicates poor binders [21]. The known PAR1 receptor antagonist Vorapaxar had a higher NNScore (Model 1), thus having a good predicted K_d within the pM concentration (Vorapaxar = 9.877 ± 2.046 ; $K_d = 132.86 \text{ pM}$). But, surprisingly, another known antagonist of PAR1, Atopaxar, had the lowest NNScore (Atopaxar = 6.219 ± 2.678 ; $K_d = 603.31 \text{ nM}$). Our new test compounds, XT5 and XT2B, also have quite good NNScores, with K_d concentrations in nM ranges (XT5 = 7.590 ± 2.767 ; $K_d = 25.70 \text{ nM}$, XT2B = 7.779 ± 3.618 ; $K_d = 16.63 \text{ nM}$). Although Artesunate has a good Vina docking score, Artesunate's NNScore is lower than our novel ligands, thus it has a higher K_d concentration (Artesunate = 6.976 ± 1.517 ; $K_d = 105.58 \text{ nM}$). Re-score values for all of the ligands have predicted that K_d values less than $25 \mu\text{M}$ indicate that all of the ligands are good binders to the PAR1 receptor. Based on the NNScore and predicted K_d , our novel molecules have the ability to be good binders against the PAR1 receptor, from the best of which is Atopaxar, making them encouraging as new promising antagonists.

The estimation of free energy of binding is an important factor in structure-based drug design. In this study, we utilized the HYDE scoring function developed on a basis of the description of hydrogen bonding and dehydration energy properties in protein–ligand complexes to predict the Gibbs free energy (ΔG), ligand efficiency and estimation of the inhibition concentration. In basic principle, the HYDE scoring function calculates the energetics of desolvation using certain parameters, such as local hydrophobicity, solvent accessible area and contact surface area, to optimize binding affinity. Thus, it can be used to calculate the atomic level of the energetically favourable and unfavourable contributions to the particular binding affinity of protein–ligand complexes. Hydration and desolvation properties are estimated using octanol/water partition coefficients of small molecules [22].

The free energy, ligand efficiency and estimation of inhibition concentration were calculated using HYDE for the best-docked pose of all ligands against the PAR1 receptor (Table 6). Known PAR1 antagonists, Vorapaxar and Atopaxar, have higher free energy scores among other ligands: -46 kJ/mol and -44.0 kJ/mol , respectively. Thus, they have higher ligand efficiency and strong inhibition concentration in the nM range. The Artesunate result is very surprising, because it shows positive free energy (11.00 kJ/mol) with a poor ligand efficiency score and inhibition concentration. Our test compounds XT5 and XT2B have shown significant results with negative free energy estimations (XT5 = -18.0 kJ/mol ; XT2B = -18.0 kJ/mol) and they also have existing good ligand efficiency scores and possess inhibition concentrations in the μM ranges. The estimate that HYDE provides in Table 6 in terms of free energy is used for predicting the binding affinity of the ligand against its receptor.

Mathematically speaking, ligand efficiency can be described as the ratio of Gibbs free energy (ΔG) to the number of heavy atoms within the compound

$$LE = (\Delta G/n)$$

Table 6. Estimation of free energy using the HYDE calculation.

Number	Ligands	Free energy ΔG (kJ/mol)	Ligand efficiency (LE)	Inhibition estimation (concentration)
1	Vorapaxar	-46.0	0.30	nM
2	Atopaxar	-44.0	0.28	nM
3	Artesunate	11.0	0.00	mM
4	XT5	-18.0	0.21	μM
5	XT2B	-18.0	0.21	μM

where $\Delta G = -RT\ln K_i$ and n is the number of heavy atoms or non-hydrogen atoms [35]. The ligand efficiency value is proportional with the free energy value. According to Table 6, all compounds with a large Gibbs free energy estimate, such as known PAR1 antagonists (Vorapaxar and Atopaxar) and our test compounds (XT2B and XT5), have good ligand efficiency values ($LE > 0$). The positive value of free energy for Artesunate caused penalties from many unfavourable interactions within the PAR1 binding pockets, making its ligand efficiency not reliable as that of the PAR1 antagonist.

In summary, the binding poses of XT2B and XT5 with the PAR1 receptor show that they are stabilized by important hydrogen bond interactions with TYR337 (Figure 1(f), (g)). Their NNScore and HYDE scoring function also gave good results, suggesting their possible high binding affinity. These docking results reveal an insight about the mechanism of these new test molecules, XT5 and XT2B, for describing their significant PAR1 antagonist activity at lower IC_{50} concentrations.

4. Conclusions

Protease-activated receptor 1 (PAR1) has been established as a promising target in many diseases, including various cancers. It belongs to the G-protein-coupled receptors (GPCRs), which mediate cellular response to specific proteases [8–10]. PAR1 plays a significant role in various pathophysiological processes including cancer; therefore, PAR1 antagonists could be very promising as a new generation of antitumor agents.

PAR1 is a unique mechanism, promising to be a novel therapeutic target for halting the progression of invasive and metastatic cancers. The results that we obtained from our in silico analysis may be useful for identifying possible novel compounds that may interact with PAR1 and hence modulate its activity as an antagonist. The in vitro activity test results have shown that our new test compounds, XT5 and XT2B, exhibited significant PAR1 antagonist activity while possessing lower IC_{50} concentrations, showing a unique interaction with TYR337 in the receptor binding site, which might have an important role in PAR1 inhibition. However, further experimental studies may be required to improve the specificity and binding affinity of these compounds against PAR1.

References

- [1] T.K. Vu, D.T. Hung, V.I. Wheaton, and S.R. Coughlin, *Molecular cloning of a functional thrombin receptor reveals a novel proteolytic mechanism of receptor activation*, Cell 64 (1991), pp. 1057–1068.
- [2] H. Turm, M. Maoz, V. Katz, Y.J. Yin, S. Offermanns, and R. Bar-Shavit, *Protease-activated receptor-1 (PAR1) acts via a novel Galpha13-dishevelled axis to stabilize beta-catenin levels*, J. Biol. Chem. 285 (2010), pp. 5137–5148.
- [3] S.R. Coughlin, *Thrombin signalling and protease-activated receptors*, Nature 407 (2000), pp. 258–264.
- [4] P.J. O'Brien, M. Molino, M. Kahn, and L.F. Brass, *Protease activated receptors: Theme and variations*, Oncogene 20 (2001), pp. 1570–1581.
- [5] F. Gieseler, H. Ungefroren, U. Settmacher, M.D. Hollenberg, and R. Kaufmann, *Proteinase-activated receptors (PARs) – focus on receptor-receptor-interactions and their physiological and pathophysiological impact*, Cell Commun. Signal. 11 (2013), pp. 86.
- [6] T.K. Vu, V.I. Wheaton, D.T. Hung, I. Charo, and S.R. Coughlin, *Domains specifying thrombin-receptor interaction*, Nature 353 (1991), pp. 674–677.
- [7] J. Chen, M. Ishii, L. Wang, K. Ishii, and S.R. Coughlin, *Thrombin receptor activation. Confirmation of the intramolecular tethered liganding hypothesis and discovery of an alternative intermolecular liganding mode*, J. Biol. Chem. 269 (1994), pp. 16041–16045.

- [8] H.W. Chu, C.W. Cheng, W.C. Chou, L.Y. Hu, H.W. Wang, C.N. Hsiung, H.M. Hsu, P.E. Wu, M.F. Hu, C.Y. Shen, and J.C. Yu, *A novel estrogen receptormicroRNA 190a-PAR-1-pathway regulates breast cancer progression, a finding initially suggested by genome-wide analysis of loci associated with lymph-node metastasis*, *Hum. Mol. Genet.* 23 (2014), pp. 355–367.
- [9] V. Gratio, N. Beaufort, L. Seiz, G.D. Virca, M. Debela, N. Grebenchtchikov, V. Magdolen, and D. Darmoul, *Kallikrein-related peptidase 4: A new activator of the aberrantly expressed protease-activated receptor 1 in colon cancer cells*, *Am. J. Pathol.* 176 (2010), pp. 1452–1461.
- [10] C.H. Chay, C.R. Cooper, J.D. Gendernalik, S.M. Dhanasekaran, A.M. Chinnaiyan, M.A. Rubin, A.H. Schmaier, and K.J. Pienta, *A functional thrombin receptor (PAR1) is expressed on bone-derived prostate cancer cell lines*, *Urology* 60 (2002), pp. 760–765.
- [11] B. Barlogie, J.D. Shaughnessy, E. Tian, and Y. Zhou, *Copy number variant-dependent genes as diagnostic tools, predictive biomarkers and therapeutic targets*, US patent 20130209446. 2013.
- [12] N. Han, K. Jin, K. He, J. Cao, and L. Teng, *Protease-activated receptors in cancer: A systematic review*, *Oncol. Lett.* 2 (2011), pp. 599–608.
- [13] J. Bangham, *Moving PARts*, *Nat. Rev. Cancer* 5 (2005), pp. 247.
- [14] M.T. García-Lopez, M. Gutierrez-Rodríguez, and R. Herranz, *Thrombin-activated receptors: Promising targets for cancer therapy*, *Curr. Med. Chem.* 17 (2010), pp. 109–128.
- [15] E. Tian, S. Usmani, Y. Zhou, B. Barlogie, and J.D. Shaughnessy, *Thrombin-induced PAR1 signaling pathway modulates β -catenin in the transformation of symptomatic myeloma cells into the quiescent phenotype*, ASH Workshop, 2011, San Diego, CA, USA.
- [16] H. Turm, M. Maoz, V. Katz, Y.J. Yin, S. Offermanns, and R. Bar-Shavit, *Protease-activated receptor-1 (PAR1) acts via a novel G α 13-dishevelled axis to stabilize β -catenin levels*, *J. Biol. Chem.* 285 (2010), pp. 15137–15148.
- [17] P.J. Morin, *Beta-catenin signaling and cancer*, *BioEssays* 21 (1999), pp. 1021–1030.
- [18] W.L. Jorgensen, *The many roles of computation in drug discovery*, *Science* 303 (2004), pp. 813–1818.
- [19] X.Y. Meng, H.X. Zhang, M. Mezei, and M. Cui, *Molecular docking: A powerful approach for structure-based drug discovery*, *Curr. Comput. Aided Drug Des.* 7 (2011), pp. 146–157.
- [20] O. Trott and A.J. Olson, *AutoDock Vina: Improving the speed and accuracy of docking with a new scoring function, efficient optimization and multithreading*, *J. Comp. Chem.* 31 (2010), pp. 455–461.
- [21] J.D. Durrant and J.A. McCammon, *NNScore: A neural-network-based scoring function for the characterization of protein-ligand complexes*, *J. Chem. Inf. Model.* 50 (2010), pp. 1865–1871.
- [22] N. Schneider, G. Lange, S. Hindle, R. Klein, and M.A. Rarey, *Consistent description of hydrogen bond and dehydration energies in protein-ligand complexes: Methods behind the HYDE scoring function*, *J. Chem. Inf. and Model.* 2012.
- [23] T. Ertan, I. Yildiz, S. Ozkan, O. Temiz-Arpaci, F. Kaynak, I. Yalcin, E. Aki-Sener, and U. Abbasoglu, *Synthesis and biological evaluation of new N-(2-hydroxy-4(or 5)- nitro/aminophenyl)benzamides and phenylacetamides as antimicrobial agents*, *Bioorg. Med. Chem.* 15 (2007), pp. 2032–2044.
- [24] T. Ertan, I. Yildiz, B. Tekiner-Gulbas, K. Bolelli, O. Temiz-Arpaci, S. Ozkan, F. Kaynak, I. Yalcin, and E. Aki, *Synthesis, biological evaluation and 2D-QSAR analysis of benzoxazoles as antimicrobial agents*, *Eur. J. Med. Chem.* 44 (2009), pp. 501–510.
- [25] Y. Musdal, T. Ertan-Bolelli, K. Bolelli, S. Yilmaz, D. Ceyhan, U. Hegazy, B. Mannervik, and Y. Aksoy, *Inhibition of human glutathione transferase P1-1 by novel benzazole derivatives*, *Turkish J. Biochem.* 37 (2012), pp. 431–436.
- [26] C. Zhang, Y. Srinivasan, D.H. Arlow, J.J. Fung, D. Palmer, Y. Zheng, H.F. Green, A. Pandey, R.O. Dror, D.E. Shaw, W.I. Weis, S.R. Coughlin, and B.K. Kobilka, *High-resolution crystal structure of human protease-activated receptor 1*, *Nature* 492 (2012), pp. 387–392.
- [27] J.J. Irwin, T. Sterling, M.M. Mysinger, E.S. Bolstad, and R.G. Coleman, *ZINC: A free tool to discover chemistry for biology*, *J. Chem. Inf. Model.* 52 (2012), pp. 1757–1768.
- [28] Dassault Systèmes BIOVIA, *Discovery Studio Modeling Environment*, Release 3.5, Dassault Systèmes, San Diego, 2012.

- [29] D. Seeliger and B.L. de Groot, *Ligand docking and binding site analysis with PyMOL and Autodock/Vina*, J. Comput.-Aided Mol. 24 (2010), pp. 417–422.
- [30] The PyMOL Molecular Graphics System, Version 1.7.4, Schrödinger, LLC, 2011.
- [31] C.A. Lipinski, F. Lombardo, B.W. Dominy, and P.J. Feeney, *Experimental and computational approaches to estimate solubility and permeability in drug discovery and development settings*, Adv. Drug Delivery Rev. 23 (1997), pp. 2–25.
- [32] D.F. Veber, S.R. Johnson, H.-Y. Cheng, B.R. Smith, K.W. Ward, and K.D. Kopple, *Molecular properties that influence the oral bioavailability of drug candidates*, J. Med. Chem. 45 (2002), pp. 2615–2623.
- [33] H. Kubinyi, *Hydrogen bonding: The last mystery in drug design?*, in *Pharmacokinetic Optimization in Drug Research: Biological, Physicochemical, and Computational Strategies*, B. Testa, H. van de Waterbeemd, G. Folkers, R. Guy, eds., Wiley Publishers, Zürich, 2007, pp. 513–524.
- [34] T. Schulz-Gasch and M. Stahl, *Scoring functions for protein-ligand interactions: A critical perspective*, Drug DiscoV. Today: Technol. 1 (2004), pp. 231–239.
- [35] A.L. Hopkins, G.M. Keserü, P.D. Leeson, D.C. Rees, and C.H. Reynolds, *The role of ligand efficiency measures in drug discovery*, Nature Rev. Drug Disc. 13 (2015), pp. 105–121.